Environmental Science and Ecotechnology 15 (2023) 100239

Contents lists available at ScienceDirect

Environmental Science and Ecotechnology

journal homepage: www.journals.elsevier.com/environmental-science-and-ecotechnology/

Original Research

Co-digestion of food waste and hydrothermal liquid digestate: Promotion effect of self-generated hydrochars

Mingshuai Shao, Chao Zhang, Xue Wang, Ning Wang, Qindong Chen, Guangyu Cui, Qiyong Xu*

Shenzhen Engineering Laboratory for Eco-efficient Recycled Materials, School of Environment and Energy, Peking University Shenzhen Graduate School, Nanshan District, Shenzhen, 518055, PR China

ARTICLE INFO

Article history:
Received 20 July 2022
Received in revised form
5 January 2023
Accepted 6 January 2023

Keywords:
Anaerobic co-digestate
Electron transfer
Food waste
Hydrothermal treatment
Microbial community
Self-generated hydrochars

ABSTRACT

Hydrothermal treatment (HTT) can efficiently valorize the digestate after anaerobic digestion. However, the disposal of the HTT liquid is challenging. This paper proposes a method to recover energy through the anaerobic co-digestion of food waste and HTT liquid fraction. The effect of HTT liquid recirculation on anaerobic co-digestion performance was investigated. This study focused on the self-generated hydrochars that remained in the HTT supernatant after centrifugation. The effect of the self-generated hydrochars on the methane (CH_4) yield and microbial communities were discussed. After adding HTT liquids treated at 140 and 180 °C, the maximum CH_4 production increased to 309.36 and 331.61 mL per g COD, respectively. The HTT liquid exhibited a pH buffering effect and kept a favorable pH for the anaerobic co-digestion. In addition, the self-generated hydrochars with higher carbon content and large oxygen-containing functional groups remained in HTT liquid. They increased the electron transferring rate of the anaerobic co-digestion. The increased relative abundance of *Methanosarcina*, Syntrophomonadaceae, and Synergistota was observed with adding HTT liquid. The results of the principal component analysis indicate that the electron transferring rate constant had positive correlationships with the relative abundance of *Methanosarcina*, Syntrophomonadaceae, and Synergistota. This study can provide a good reference for the disposal of the HTT liquid and a novel insight regarding the mechanism for the anaerobic co-digestion.

1. Introduction

With increasing food waste and the widespread use of anaerobic digestion techniques, large amounts of digestate of food waste (DFW) are being generated. Approximately 0.57–1.34 t DFW is estimated to be generated after one-ton food waste treatment [1]. Large-scale generation of DFW, which is rich in nutrients and pathogens, is associated with several environmental and safety concerns [2–4]. In addition, because DFW has a high-water content and low dewaterability, its storage, transportation, and post-treatment are expensive [5]. Recently, hydrothermal treatment (HTT) has rapidly emerged as a highly efficient method to dispose of the DFW [6]. Hydrothermal treatment has been widely used because it can improve the dewaterability and resource recovery of the DFW [7,8].

In HTT processes, the undigested organic matter after anaerobic digestion and microorganisms are decomposed and transferred to the liquid fraction [9]. The solid can be separated easily due to the binding between the water, and the solid is broken down during HTT [10,11]. However, HTT technology still exhibits several challenges, such as the treatment of the waste liquid product and high energy consumption [12]. The HTT liquid fraction contains high amounts of volatile fatty acids (VFAs), sugars, and other hemicellulosic carbohydrates. Directly using this liquid as a liquid fertilizer for farmland irrigation may lead to nitrogen volatilization and over-fertilization [13,14]. Our previous study showed that recirculating the HTT liquid in the anaerobic digestion process is a promising strategy for decreasing the amount of liquid post-treatment and HTT energy cost [9].

Notably, because of the complex characteristics of the HTT liquid, the effect of the liquid recirculation on CH_4 production is

* Corresponding author.
E-mail address: qiyongxu@pkusz.edu.cn (Q. Xu).

https://doi.org/10.1016/j.ese.2023.100239

unpredictable. During HTT, reactions such as hydrolysis, dehydration, and polymerization occur at different temperatures [15]. The hydrolysis reaction in the HTT accelerates the solubilization of the polymers and increases the soluble chemical oxygen demand (sCOD) contents of the HTT liquid fraction, thereby promoting CH_4 production [16,17]. In contrast, the lignin decomposition products (such as phenols) and carbohydrate dehydration products (such as furfural and furans) may lead to methanogenic inhibition [18,19]. When the HTT temperature is higher than 180 °C, Maillard reactions will occur. The products of pyrazine, pyrrole, and *N*-containing heterocyclic compounds may decrease CH_4 production [19]. Suarez et al. [19] reported that the addition of HTT liquid fraction in anaerobic digestion could result in a 41–45% reduction in CH_4 production. In this context, the role of the HTT liquid fraction on the anaerobic co-digestion needs to be clarified. Our previous study found that amounts of self-generated hydrochars with a particle size between 0.61 and 1.29 μm remained in the HTT liquid after centrifugation [15]. It is well known that hydrochars can promote organic degradation and CH_4 conversion from volatile fatty acids in the anaerobic co-digestion [20–22]. However, the hydrochars are usually prepared by a separate process and then added into the anaerobic digestion systems to improve CH_4 yield in current studies. The self-generated hydrochars remaining in the HTT liquid have usually been overlooked in previous studies but are important for condition optimization in future studies.

Considering these aspects, the DFW was treated at different HTT temperatures in this study. Batch anaerobic co-digestion of the food waste and HTT liquid fraction was performed to determine the effect of the HTT liquid on CH_4 production. The role of the self-generated hydrochars in the anaerobic co-digestion process was discussed. The findings are expected to provide novel insights regarding the mechanism of the anaerobic co-digestion of the HTT liquid fraction and food waste.

2. Material and methods

2.1. Preparation of DFW, food waste, and inoculum

The DFW was collected from a food waste treatment plant with a treatment capacity of 300 t d^{-1} in Shenzhen (Guangdong Province, China). The digestate was stored at 4 °C. Before each experiment, the digestate was conditioned back to ambient temperature and homogenized via shaking. All tests were completed within seven days after sampling.

Synthetic food waste was used in this study to improve the reproducibility of the experiments. The food waste was synthesized by mixing 30 wt% lettuce, 20 wt% pork, 20 wt% rice, 15 wt% tofu, and 15 wt% steamed bread on a wet basis, according to the previous study [23]. After homogenization, the food waste was stored at −20 °C.

The inoculum was collected from a food waste treatment plant in Shenzhen (Guangdong Province, China) and was used for anaerobic digestion experiments. Subsequently, the inoculum was cultured without nutrients until the organic matter was completely consumed and used in the anaerobic co-digestion experiments. The characteristics of the DFW, food waste and inoculum are presented in Table S1.

2.2. Hydrothermal treatment

The DFW was hydrothermally treated at 140 and 180 °C in a 1000 mL Hastelloy autoclave reactor with a stirrer (YZPR-1000 M, Shanghai, China). In each experiment, 500 mL of DFW was added to the reactor. And then, to remove the residue air, nitrogen was purged for 10 min. All the DFW was kept at the target temperature for 60 min with stirring at 300 rpm. And then, the autoclave was cooled down to ambient temperature by circulating water. The treated DFW was collected and stored at 4 °C. The HTT temperatures were selected according to our previous study [15]. When the HTT temperatures were at 140–180 °C, the best efficiency of solid-liquid separation was realized, and more than 80% of organics were transferred to the liquid. The generated HTT liquid may have the potential to co-anaerobic digestion with food waste to promote resource recovery. After the HTT process, the liquid was separated from the large-size solids via centrifugation at 4000 rpm for 30 min. The centrifugation conditions were selected according to Wakeman's research [24]. The separated liquids after centrifugation were labeled SH140 and SH180, according to the HTT temperature. The liquid separated from the raw DFW was labeled SDFW. All the liquid samples were stored in a refrigerator at 4 °C until use. The characteristics of the supernatant are summarized in Table S1.

2.3. Anaerobic co-digestion

Anaerobic digestion assays can be designed in batch or continuous mode [25]. Batch experiments have been widely used in anaerobic biodegradability, inoculum activity, and inhibition [26]. In this study, the effects of the HTT liquid on CH_4 production were investigated by referring to the batch anaerobic co-digestion experiments. The experiments were conducted in 300 mL glass serum vials. Each vial contained 10 g of food waste and 110 mL SDFW, SH140, SH180, or ultrapure water. The added liquids were SDFW, SH140, SH180, and deionized water, labeled FW-SDFW, FW-SH140, FW-SH180, and FW-Water, respectively. The FW-Water sample was used as a control. The vial contained only inoculum was set as the blank. Considering the chemical oxygen demand (COD) of the feedstock, a certain volume of inoculum was added to the vials to achieve a higher food/microorganism (F/M) of 8 g COD per g VS for all the tests [27]. The initial inoculum concentration was 1.25 g VS L^{-1}. Finally, deionized water was added to the vials to obtain a final working volume of 150 mL. A higher F/M was used to perform anaerobic digestion experiments in this study. The organic loading rate is one important factor for the anaerobic co-digestion system to convert CH_4 methane stably [28]. Whereas recycling HTT liquid containing amounts of dissolved organic matter may cause the fluctuation of organic load in the anaerobic co-digestion system. Studying the anaerobic co-digestion with a higher F/M is more meaningful. In addition, a higher F/M may prolong the process of hydrolysis, acidification, and methanation of anaerobic digestion, which facilitates timely monitoring of anaerobic co-digestion. Therefore, studying the anaerobic co-digestion with a higher food/microorganism ratio is more suitable for the actual HTT liquid recycling demand.

The vials were flushed with N_2 for 5 min to ensure anaerobic conditions. After nitrogen purging, the vials were sealed with rubber stops and metal crimps and incubated at 35 °C. All the experiments were conducted in triplicate. A volume of 3 mL biogas was sampled periodically, and the concentrations of CH_4 and CO_2 were measured. Triplicate blank samples with no substrate were used to estimate the endogenous CH_4 production during the assay. The CH_4 yield was calculated by subtracting the CH_4 endogenous output obtained from the blank inoculum sludge, and CH_4 volume at standard temperature (273 K) and pressure (1 atm) were recorded.

2.4. Analysis methods

2.4.1. Analysis of the anaerobic co-digestion products

The ratio of CH_4 production (mL) to the COD (g COD) of the substrate was used to define the CH_4 yield. Biogas from the anaerobic co-digestion, mainly including CH_4 and CO_2, was assessed by a gas chromatograph (6890, Agilent, Santa Clara, CA, USA).

A volume of 5 mL effluent was periodically sampled from the anaerobic co-digestion vials to determine the VFAs concentration, COD, sCOD, and pH. The VFAs were detected through a high-performance liquid chromatography system (1260 Infinity, Agilent, USA) with a Hi-plex H column and a refractive index detector [23]. The COD and sCOD of the anaerobic co-digestion effluent and supernatant production were determined using the standard analytical method [29]. The pH of the effluent samples from anaerobic co-digestion was measured using a pH meter (CHN868, Thermo Orion, USA).

2.4.2. Microbial community analysis

Samples were taken from the suspended sludge during the acidogenesis stage and the methanogenic stage of anaerobic co-digestion and then stored at −80 °C until analysis. The high-throughput 16S rRNA gene sequencing (Genewiz Company, China) was used to analyze the microbial community. The DNA of samples was extracted by HiPure Soil DNA Kit (Magen, USA), and the concentration of DNA was measured by the Qubit® dsDNA HS Assay Kit (ThermoFisher, USA). The extracted DNA was amplified with forward primer (CCTACGGRRBGCASCAGKVRVGAAT) and reverse primer (GGACTACNVGGGTWTCTAATCC) designed by GENEWIZ (Suzhou, China) targeting the V3 and V4 hypervariable regions of 16S rDNA gene of both bacteria and archaea. Primers and regions were selected according to the method used in Lim et al.'s research [30]. Sequencing was performed on the Illumina MiSeq/Novaseq (Illumina, USA). The VSEARCH (1.9.6) with the reference database of Silva 138 was used to realize operation taxonomic unit (OTU) clustering. The OTU species taxonomy was analyzed by the Ribosomal Database Program classifier with the Bayesian algorithm.

2.4.3. Conductivity analysis

The effect of the liquid fraction on the electron transferring activity for anaerobic digestion was determined considering the cyclic voltammetry (CV) curve. The CV curve was obtained using an electrochemical workstation (CH1760D, Chenhua, China) with a single-chamber three-electrode electrolytic cell. Graphite, platinum, and Ag/AgCl were used as the three-electrode. 70 mL of the anaerobic digestion effluents was added into the sealed electrolytic cell [27]. The scan rate was set as 40, 60, 80, 100, 120, 140, 160, 180, 200, 220, and 240 mV s^{-1}, respectively [27,31–33]. The electron transferring rate constant (k_{app}) was calculated based on equations (1) and (2) [27,33].

$$E_{pc} = E_c^0 - \left(\frac{RT}{\alpha nF}\right)\ln\left[\frac{\alpha nF\nu}{RTk_{app}}\right] \quad (1)$$

$$E_{pa} = E_a^0 - \left(\frac{RT}{(1-\alpha)nF}\right)\ln\left[\frac{(1-\alpha)nF\nu}{RTk_{app}}\right] \quad (2)$$

In the equations, α (a.u.) is the transfer efficiency; n (mol) is the number of electrons transferred; E_{pa} (V) is the oxidation peak potential; E_{pc} (V) is the reduction peak potential; E_a^0 (V) is the formal potential for anodic; E_c^0 (V) is the formal potential for cathodic; ν (V s^{-1}) is the scan rate; the value of T is 298 K; the value of R is 8.314 J mol^{-1} K^{-1}; and the value of F is 96485 C mol^{-1}. The value of α and n were calculated by equation (3):

$$\lg k_{app} = \alpha\lg(1-\alpha) + (1-\alpha)\lg\alpha - \lg\left(\frac{RT}{nF\nu}\right) - (1-\alpha)\alpha\frac{nF\Delta E}{2.303RT} \quad (3)$$

where ΔE is the difference between the value of reduction peak potential and the value of oxidation peak potential, $\Delta E = E_{pa} - E_{pc}$, (V).

2.4.4. Characterization of the self-generated hydrochars in the HTT liquid

The self-generated hydrochars were extracted from the HTT liquid fraction by filtration through a 0.22 μm filter and freeze-dried for 72 h [34]. The samples extracted from SH140 and SH180 were labeled SH140-s and SH180-s, respectively. The same procedure was conducted for the raw SDFW, and the collected solid sample was labeled as SDFW-s. The particle size distribution was analyzed using a Malvern Zeta-sizer Nano ZS (Nano-ZS90, Malvern Instruments Inc., UK). The self-generated hydrochars were subjected to a Fourier transform infrared (FTIR) analysis to determine the change in the functional groups during HTT. The spectrum of FTIR was conducted by an FTIR spectrometer (IRTracer-100, Shimadzu, Japan) with a resolution of 2 cm^{-1} over a range of 400–4000 cm^{-1}. An elemental analyzer (2400 Series II, PerkinElmer, UK) was used to determine the carbon (C), hydrogen (H), nitrogen (N), and sulfur (S) content. The oxygen (O) was calculated by difference. The surface morphology of the self-generated hydrochars was analyzed by scanning electron microscopy with an energy dispersive spectrometer (SEM-EDS, TM 4000plus, Hitachi, Japan).

2.5. Statistical analysis

Principal component analysis (PCA) is a powerful statistical tool for studying multivariate data [35]. In this study, PCA analysis was used to analyze the possible interrelation between parameters of the added liquid (deionized water, SDFW, SH140, and SH180) and their closeness to methane production at the acidogenesis and methanogenesis stages. Four predominant bacteria, four predominant archaea, and thirteen physicochemical indicators of added liquid and the performance of anaerobic co-digestion were grouped for PCA analysis. The data of anaerobic co-digestion at the 10th day (acidogenesis stage) and 56th (methanogenesis stage) day were analyzed using OriginPro 9.0 (OriginLab, USA).

3. Results and discussion

3.1. Performance of anaerobic co-digestion with different HTT liquid

3.1.1. CH_4 production

Little CH_4 was detected in FW-Water (0.17 mL per g COD), although significant CH_4 production was observed in FW-SDFW, FW-SH140, and FW-SH180 (Fig. 1a). The maximum CH_4 yield were 309.36, 331.61, and 297.82 mL per g COD for FW-SH140, FW-SH180, and FW-SDFW, respectively. The digestate liquid, especially SH140 and SH180, provided favorable conditions for food waste anaerobic digestion. The pH of FW-Water sharply decreased to 5.21 in the anaerobic co-digestion process (Fig. S1). The decrease in the pH inhibited bacterial activity and CH_4 conversion. The pH of FW-SDFW, FW-SH140, and FW-SH180 was maintained at approximately 7.2 (Fig. S1), which is highly favorable for methanogen metabolism and growth [36].

Two peaks were observed in the CH_4 production rate curves of

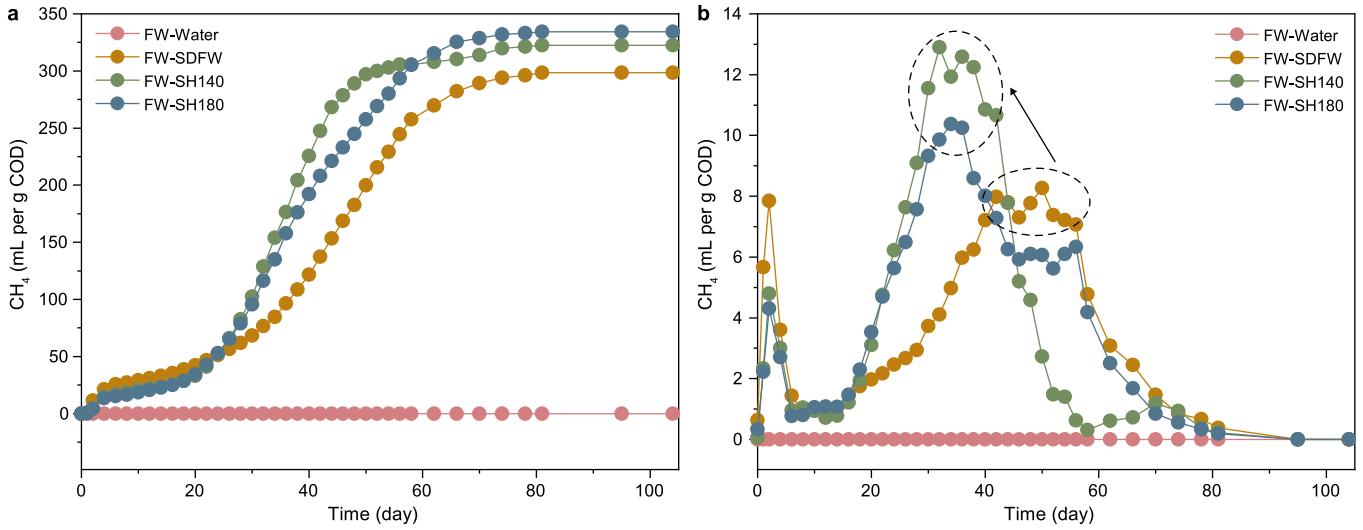

Fig. 1. The CH_4 production yield (**a**) and rate (**b**) under the different addition of HTT liquid. FW-SDFW, FW-SH140, FW-SH180, and FW-Water represent the anaerobic co-digestion of food waste with food waste digestate liquid, food waste digestate liquid after hydrothermal treatment at 140 °C, and food waste digestate liquid after hydrothermal treatment at 180 °C, respectively.

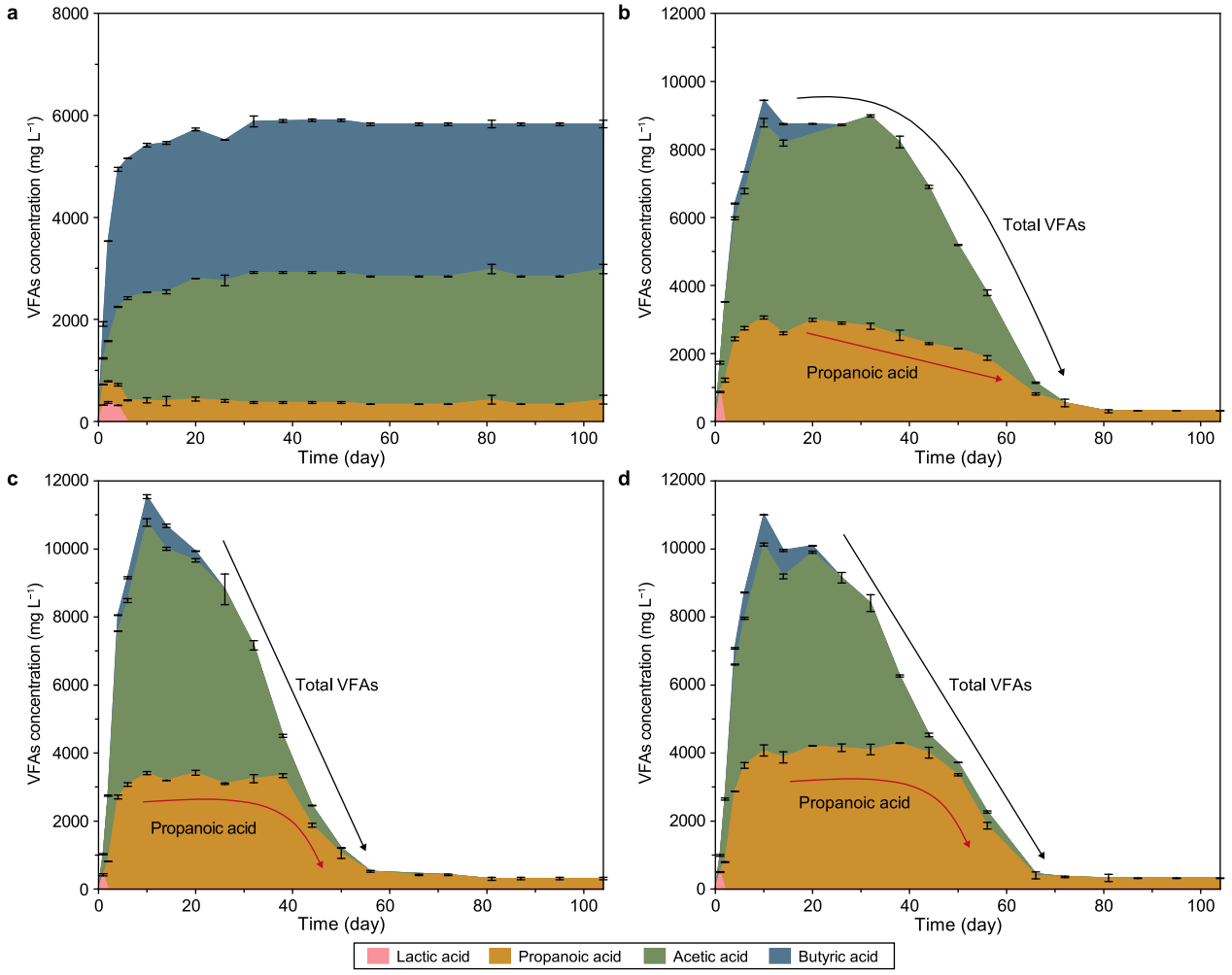

Fig. 2. **a**, Evolution of fatty acids composition during the anaerobic digestion of FW-Water. **b**–**d**, Evolution of fatty acids composition during the anaerobic digestion of food waste supplemented with SDFW (**b**), SH140 (**c**), and SH180 (**d**). FW-SDFW, FW-SH140, FW-SH180, and FW-Water represent the anaerobic co-digestion of food waste with food waste digestate liquid, food waste digestate liquid after hydrothermal treatment at 140 °C, and food waste digestate liquid after hydrothermal treatment at 180 °C, respectively.

Table 1
COD balance of anaerobic co-digestion under different conditions. FW-SDFW, FW-SH140, FW-SH180, and FW-Water represent the anaerobic co-digestion of food waste with food waste digestate liquid, food waste digestate liquid after hydrothermal treatment at 140 °C, and food waste digestate liquid after hydrothermal treatment at 180 °C, respectively.

Substrate	Beginning of anaerobic co-digestion			End of anaerobic co-digestion		
	COD proportion of food waste (g)	COD proportion of liquid fraction (g)	COD proportion of inoculum (g)[a]	COD proportion of biogas (g)	COD proportion of supernatant (g)	COD proportion of residue (g)
FW-Water	2.91	0.00	0.04	0.46	1.84	0.65
FW-SDFW	2.91	0.72	0.09	2.63	0.71	0.36
FW-SH140	2.91	1.35	0.14	3.44	0.53	0.43
FW-SH180	2.91	1.44	0.15	3.57	0.62	0.30

[a] The volume of inoculum was added in vials based on the COD of the feedstock.

FW-SDFW, FW-SH140, and FW-SH180 (Fig. 1b). The first peak was observed during the first six days, attributable to the utilization of the residual VFAs from the food waste treatment plant. As the anaerobic digestion progressed, the macromolecular VFAs degraded to small molecular VFAs by the beta-oxidation process and were then converted to CH_4, leading to the second CH_4 generation peak [23]. The second peaks of FW-DFW, FW-H140, and FW-H180 appeared on days 50, 34, and 34, with peak values of 8.27, 12.59, and 10.37 mL per g COD per day, respectively. The HTT liquids promoted organic matter degradation and CH_4 production compared to the raw digestate. Although FW-SH140 had a higher CH_4 production rate (Fig. 1b) than FW-SH180, the final cumulative CH_4 production of FW-SH140 was lower than that of FW-SH180. The compounds generated at 180 °C could delay CH_4 production but did not considerably influence the final CH_4 yield.

In our previous study, the energy balance of recirculating the HTT liquid in the anaerobic digestion process was elaborately discussed [9]. The energy recovered from the HTT liquid via anaerobic digestion will compensate for most heating energy consumption during the DFW hydrothermal process. The values of net energy consumption were 33.85 MJ per t DFW during the whole treatment process with HTT pretreatment but 124.75 MJ per t DFW without HTT pretreatment. Therefore, recirculating the HTT liquid in the anaerobic co-digestion process is promising for wastewater treatment and resource recovery.

3.1.2. VFAs production

The VFAs concentrations during the anaerobic co-digestion with or without the SDFW, SH140, and SH180 supernatants were significantly different (Fig. 2). In the anaerobic digestion process involving FW-Water, the total VFAs concentration sharply increased to 5000 mg L^{-1} in the first ten days, then gradually increased to 6000 mg L^{-1} in the following 20 d, and exhibited a stable value at the end of the anaerobic co-digestion process (Fig. 2a). In contrast, the total VFAs concentration in the FW-SDFW, FW-SH140, and FW-SH180 samples decreased after it was maximized, corresponding to an increase in CH_4 production. The accumulation of VFAs has been noted to inhibit anaerobic digestion when its concentration exceeds 3500 mg L^{-1} [36]. The highest total concentrations of VFAs in the samples with FW-SDFW, FW-SH140, and FW-SH180 were 9,439, 11,536, and 11,003 mg L^{-1}, respectively, but no methanogenesis inhibition was observed. This observation could be attributed to the buffer effect of the SDFW and HTT liquids. Because the methanogenesis process was not inhibited, the VFAs rapidly converted to CH_4.

In addition, the compositions of the VFAs in FW-Water, FW-SDFW, FW-SH140, and FW-SH180 were different. In the control sample (FW-Water), butyric acid was the primary VFA, followed by acetic acid and propionic acid. In contrast, acetic acid was the dominant VFA in the FW-SDFW (Fig. 2b), FW-SH140 (Fig. 2c), and FW-SH180 (Fig. 2d) samples in the first 26 days, although traces of butyric acid were detected. The addition of SDFW, SH140, and SH180 changed the conversion route of the organic matter in the anaerobic co-digestion system. Moreover, the addition of SH140 and SH180 changed the utilization order of the different VFAs. In the FW-SDFW, the VFAs concentration plateaued, indicating the

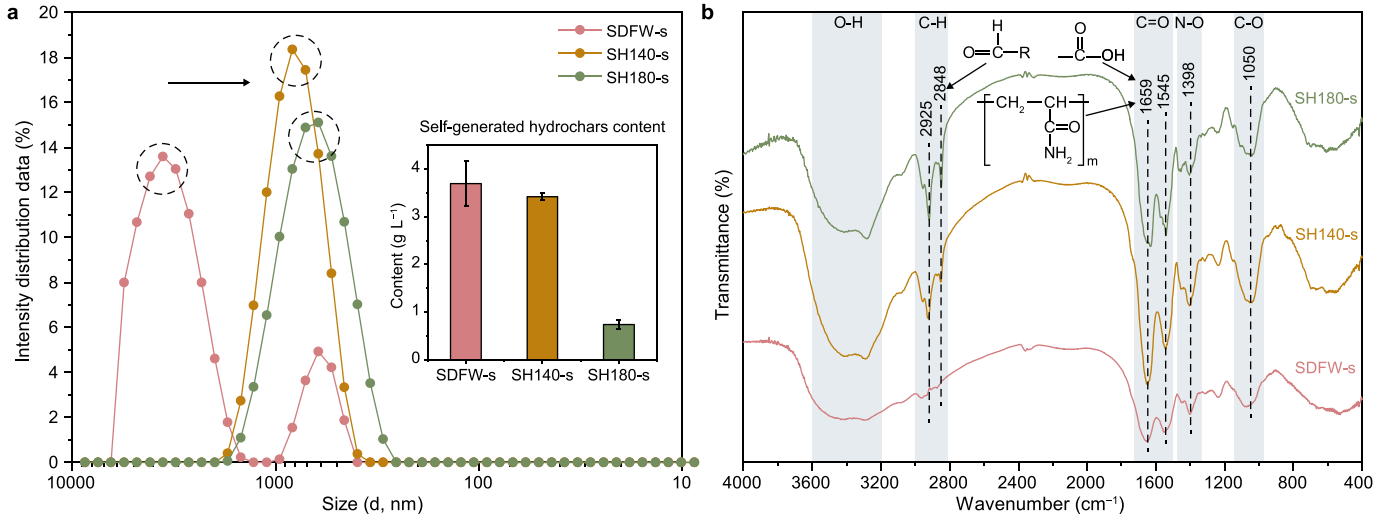

Fig. 3. **a**, The particle size distribution and the contents. **b**, FTIR spectra of SDFW-s, SH140-s, and SH180-s. SDFW-s, SH140-s, and SH180-s represent the small-size particles from food waste digestate liquid, food waste digestate liquid after hydrothermal treatment at 140 °C, and food waste digestate liquid after hydrothermal treatment at 180 °C, respectively.

balance between acid production and VFAs consumption [37]. In the FW-SH140 and FW-SH180 samples, the contents of acetic acid rapidly decreased after reaching their maximum value near day 10.

3.1.3. COD balance

The COD balance at the beginning and end of the anaerobic co-digestion was calculated (Table 1) to examine the efficiency of the organic matter utilization [38]. At the beginning of the anaerobic co-digestion, most of the COD in the FW-Water was contributed by the prepared food waste. In the FW-SDFW, FW-SH140, and FW-SH180 sample bottles, the added liquid provided 0.72, 1.35, and 1.44 g of COD, respectively. The digestate and HTT liquid promoted the conversion of the organic matter in the food waste and liquid to CH_4. As shown in Table 1, the COD contributed by the biogas accounted for 2.63, 3.44, and 3.57 g of COD for the FW-SDFW, FW-SH140, and FW-SH180 samples, respectively. After anaerobic co-digestion, the COD proportion contributed by the biogas in the control sample (FW-Water) was only 0.46 g. Most organic matter (2.49 g of COD) remained in the supernatant and solid residue, indicating that CH_4 conversion was interrupted in the control sample. At the same time, fewer COD remained in supernatant or residue after anaerobic digestion in FW-SDFW, FW-SH140, and FW-SH180 sample bottles. The COD balance results indicated that the HTT liquid promoted the CH_4 conversion of food waste during the anaerobic co-digestion, and SH180 corresponded to a superior effect. The COD balance was consistent with the results of CH_4 production and VFAs concentration.

3.2. Effect of the self-generated hydrochars on electron transferring activity

3.2.1. The characteristics of the self-generated hydrochars

The characteristics of the self-generated hydrochars were analyzed, including particle size distribution, elementary substance, and surface functional groups, to explore their effects on promoting anaerobic co-digestion. The SDFW-s and the self-generated hydrochars (SH140-s and SH180-s) obtained from SDFW, SH140, and SH180 were characterized to explore their effect on promoting anaerobic co-digestion. As shown in Fig. 3a, the solid particle content in the raw digestate liquid was 3.70 g L^{-1}, and the average solid particle size was 5.96 μm. HTT at a temperature of 140 °C did not considerably influence the solid particle content but decreased the particle size to 1.0 μm, indicating the large particles' disintegration. When the HTT temperature increased to 180 °C, the solid particle content decreased to 0.74 g L^{-1}, and the particle size decreased to 0.75 μm because more complicated reactions, including hydrolysis and decomposition, occurred [15,17]. The small size of the self-generated hydrochars will help them to be dispersed in the anaerobic digestion system and improve the methanogenic performance.

The HTT process had little effect on the morphological structures of the particles (Fig. S2) but affected the elemental composition significantly. The C content of the SDFW-s was only 35.05% (Table 2), while it increased to 41.27% and 41.46% for SH140-s and SH180-s, respectively, indicating carbonization occurred during HTT [15]. The carbon contents of self-generated hydrochars (SH140-s and SH180-s) are much higher than that of the reported hydrochars (24–35%) [39–41]. In addition, SH140-s and SH180-s contained less ash content, which was 10.10% and 18.85%, respectively. The higher C content and lower ash content are preferred characteristics of hydrochars to promote the anaerobic co-digestion performance.

Table 2
The elemental composition of SDFW-s, SH140-s, and SH180-s. SDFW-s, SH140-s, and SH180-s represent the small-size particles from food waste digestate liquid, food waste digestate liquid after hydrothermal treatment at 140 °C, and food waste digestate liquid after hydrothermal treatment at 180 °C, respectively.

Sample	C (%)	H (%)	N (%)	S (%)	O (%)	Ash (%)
SDFW-s	35.05	4.22	7.35	1.00	42.58	9.80
SH140-s	41.27	4.13	7.60	1.01	35.89	10.10
SH180-s	41.46	3.80	6.98	1.66	27.24	18.85

The surface functional groups of SDFW-s, SH140-s, and SH180-s were analyzed by FTIR analysis (Fig. 3b). The bands in the range of 3600–3200 cm^{-1} corresponded to the stretching of C–OH. The increase in the C–OH relative abundance in SH140-s and SH180-s was attributed to the decomposition and hydrolysis reactions. At the same time, the band strength of C–OH of SH180-s was lower than it was in SH140-s. This may be due to the dehydration reaction occurring at 180 °C [42]. The bands at 1659 and 1545 cm^{-1} corresponded to the vibration of C=O, and the bands at 1050 cm^{-1} corresponded to the vibration of C–O [20]. DFW is mainly composed of proteins, polysaccharides, lignin, and other organic compounds [9,43]. During a low-temperature HTT process, decomposition and hydrolysis are the dominant reactions [9]. Therefore, the self-generated hydrochars have a higher content of oxygen-containing functional groups than SDFW-s. With the increase in HTT temperature, the dehydration and decarboxylation were strengthened gradually [44]. Therefore, the content of oxygen-containing functional groups in SH180-s was lower than that in SH140-s. The abundant oxygen-containing functional groups and the small size of the self-generated hydrochars will help them to be dispersed in the anaerobic digestion system and improve the methanogenic performance.

In general, the surface oxygen-containing functional groups can donate and accept electrons, thereby activating the redox reaction of hydrochars to facilitate direct interspecies electron transfer during the anaerobic co-digestion process [20,45,46]. The higher abundance of surface oxygen-containing functional groups in SH140-s and SH180-s was consistent with their higher capacity to promote CH_4 production (Fig. 1). In addition, the surface oxygen-containing functional groups in the self-generated hydrochars from SH140 and SH180 could adsorb the VFAs and retard the acid inhibition in the food waste anaerobic digestion [47]. Consequently, although the VFAs concentrations in SH140-s and SH180-s were considerably higher than 3500 mg L^{-1}, no acid inhibition was observed.

3.2.2. The variation of electron transferring activity

The electron transfer intensity between bacteria and archaea considerably influences anaerobic digestion characteristics [48]. Cyclic voltammetry is commonly used to describe the electron transport properties of anaerobic digestion systems by analyzing the dependence of the peak currents on the scan rates [27,31,33]. The favorable anaerobic digestion environment of electron transferring performance will help to promote cooperation between microbes [33]. The CV curves were analyzed to investigate the effect of the self-generated hydrochars on electron transport. As shown in Fig. 4a–c, the peak currents (peaks 1 and 2) of SDFW, SH140, and SH180 increased with the increasing scan rate. The relationship of Ep-E_0 with lnV was used to express the variation in the voltage with the scan rate. The k_{app} of SH140 (2.08×10^{-3} s^{-1}) and SH180 (3.10×10^{-3} s^{-1}) were 17.91 and 27.18 times that of SDFW (1.09×10^{-4} s^{-1}), respectively (Fig. 4d). The k_{app} in FW-SDFW, FW-SH140, and FW-SH180 was 2.54×10^{-4}, 2.47×10^{-3}, and 6.76×10^{-3} s^{-1}, respectively (Fig. 4d). This calculation highlighted that the HTT improved the electron transferring activity of the digestate, and the addition of SH140 and SH180 increased the electron transferring rate of the anaerobic co-digestion system. The higher k_{app} in FW-SH140 and FW-SH180 promoted syntrophic

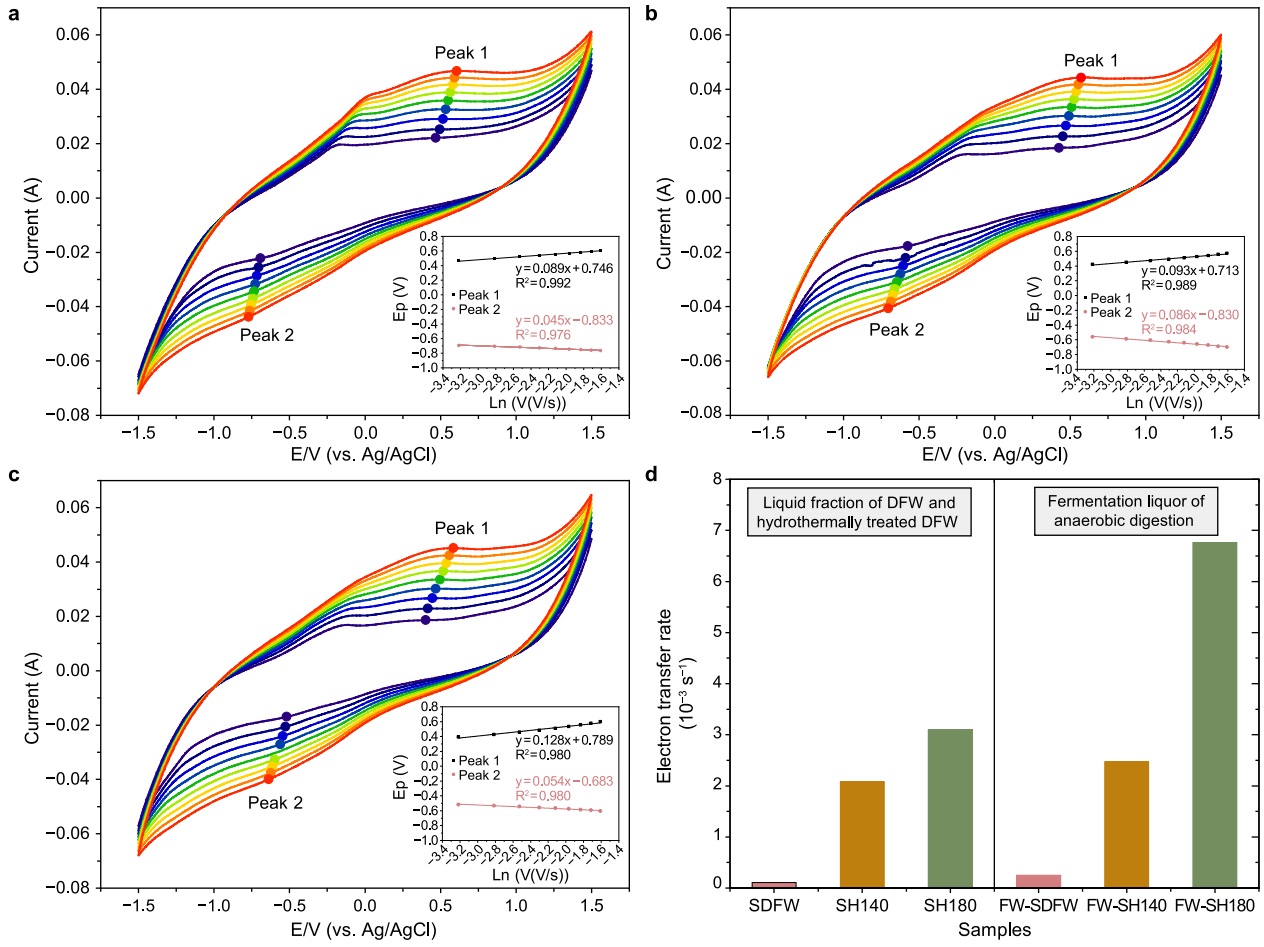

Fig. 4. **a**–**c**, Cyclic voltammetry curves at diverse scan rates of 40, 60, 80, 100, 120, 140, 160, 180, 200, 220, and 240 mV s^{-1} and the logarithm functions of the scan rates and peak potentials of SDFW-s (**a**), SH140-s (**b**), and SH180-s (**c**). **d**, Electron transferring rates of the liquid fraction and anaerobic co-digestion slurry. SDFW-s, SH140-s, and SH180-s represent the small-size particles from food waste digestate liquid, food waste digestate liquid after hydrothermal treatment at 140 °C, and food waste digestate liquid after hydrothermal treatment at 180 °C, respectively.

relationships, which is associated with increased CH_4 production efficiency [31]. The microbial community was discussed in the next section.

3.3. Microbial community composition of different anaerobic co-digestion stages

3.3.1. Bacterial community composition

The changes in the VFAs and CH_4 production with the addition of SDFW, SH140, and SH180 led to variations in the community structure of the microbes during FW-Water. Molecular biological measures with next-generation sequencing techniques were used to extract information regarding the microbial communities in the anaerobic digestion process of inoculum, FW-Water, FW-SDFW, FW-SH140, and FW-SH180 [38]. The alpha diversity indices were shown in Table S2, including ACE, Chao1, OTUs, Shannon, and Simpson. The alpha of FW-SDFW, FW-SH140, and FW-SH180 was considerably higher than those of FW-Water and inoculum, indicating that the ecological functions of the bacterial community during the acidogenesis and methanogenesis stages were strengthened by SDFW, SH140, and SH180 [49].

The community structure consisted of similar bacterial phyla, but the relative abundances varied significantly (Fig. 5). Firmicutes, Bacteroidetes, and Synergistota were the most dominant bacteria, accounting for more than 91.97% of the content in all samples. The relative abundances of Firmicutes, Bacteroidetes, and Synergistota in inoculum were 78.35%, 13.85%, and 3.74%, respectively. After the addition of the food waste, the relative abundances of Firmicutes increased to 88.34%, whereas the relative abundances of Bacteroidetes and Synergistota decreased to 8.01% and 2.06%, respectively. The SDFW, SH140, and SH180 promoted the reproduction of Bacteroidetes and Synergistota. As shown in Fig. 5, the relative abundances of Bacteroidetes were maintained at 30.39–38.33% in the acidogenesis stage, and the relative abundances of Bacteroidetes were 9.66–11.01% in the methanogenesis stage. The relative abundances of Firmicutes decreased to 55.07–70.24% in the FW-SDFW, FW-SH140, and FW-SH180.

Firmicutes are known to secrete extracellular hydrolases (such as cellulase, lipase, and protease), which can accelerate the degradation of large molecules such as cellulose, protein, and lipids [50]. The high proportion of Firmicutes in FW-Water was attributable to the lower community diversity. The nucleic acid concentration in the FW-Water was 85.4–93.7% (Fig. S3), lower than that in the other samples, indicating that most of the microorganisms could not survive in the acidic environment of FW-Water.

Bacteroidetes represents acid-forming bacteria that can be capable of converting arabinose, glucose, cellobiose, starch, and other substances into acetic acid, butyric acid, isovaleric acid, H_2, and CO_2 [51]. The increase in the abundances of Bacteroidetes in FW-SDFW, FW-SH140, and FW-SH180 during the acidogenesis

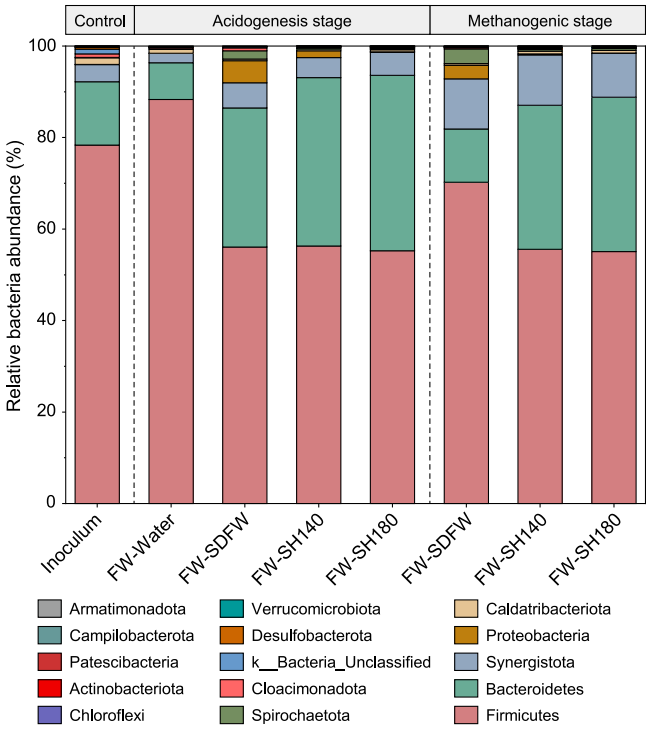

Fig. 5. Relative abundance of major bacteria (phylum level) at the acidogenesis and methanogenesis stages of anaerobic digestion. FW-SDFW, FW-SH140, FW-SH180, and FW-Water represent the anaerobic co-digestion of food waste with food waste digestate liquid, food waste digestate liquid after hydrothermal treatment at 140 °C, and food waste digestate liquid after hydrothermal treatment at 180 °C, respectively.

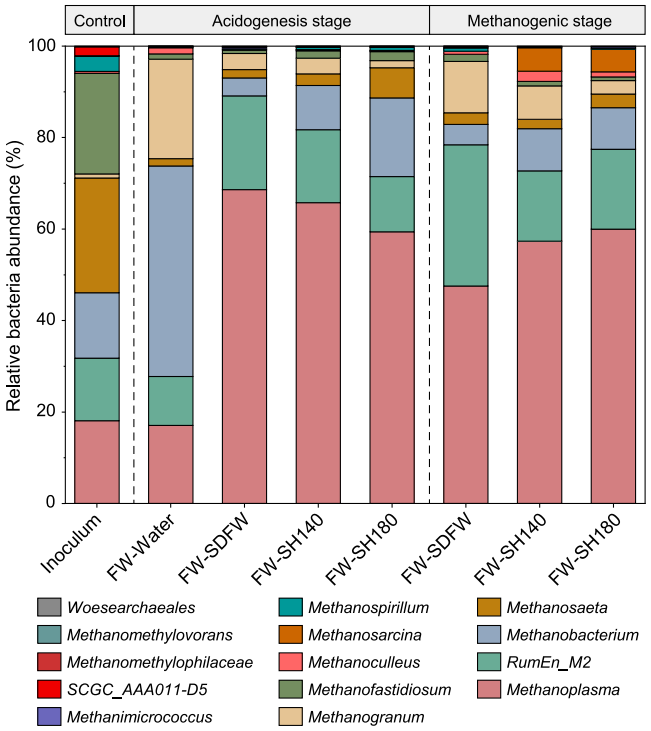

Fig. 6. Relative abundance of major archaea (genus level) at the acidogenesis and methanogenesis stages of anaerobic digestion. FW-SDFW, FW-SH140, FW-SH180, and FW-Water represent the anaerobic co-digestion of food waste with food waste digestate liquid, food waste digestate liquid after hydrothermal treatment at 140 °C, and food waste digestate liquid after hydrothermal treatment at 180 °C, respectively.

stage indicated the presence of more favorable conditions, such as the pH. In addition, the FW-SH140 and FW-SH180 could be easily biodegraded because large amounts of large molecules or refractory substances were degraded to small molecules in the HTT process before the anaerobic digestion [9]. These bacteria community results are consistent with the VFAs result (Fig. 2) and sCOD result (Fig. S4), which indicates that the generation of VFAs was related to Bacteroidetes.

Synergistota, also known as Synergistetes, represents acid-forming bacteria that can produce short-chain fatty acids and function as syntrophic acetate oxidizers [52]. In recent studies, Synergistota is an electrochemically active bacterium that can establish syntrophic metabolism with hydrogenotrophic methanogens (*Methanobacterium* and *Methanospirillum*) and participate in interspecies electron transfer [1,53]. Synergistota is expected to play a direct role in the direct interspecies electron transfer interaction of electroactive communities. The increasing relative abundances of Synergistota in FW-SDFW, FW-SH140, and FW-SH180 during the methanogenesis stage likely increased the methanogenic efficiency. The addition of SDFW, SH140, and SH180 enriched the electrochemically active bacterium (Synergistota) and enhanced the direct interspecies electron transfer. Notably, the phylum Spirochaetota was found only in FW-SDFW and not in FW-SH140 and FW-SH180. It has been noted that propionic, butyric, and valeric acid can be converted into acetic acid, H_2, and CO_2 by Spirochaetota [54]. This result may be related to the utilization of VFAs in FW-SDFW, FW-SH140, and FW-SH180.

3.3.2. Archaea community composition

As shown in Fig. 6, the relative abundances of bacteria were classified at the genus level. The community structures of inoculum, FW-Water, and FW-SDFW varied with the anaerobic digestion and HTT liquid fractions. The methanogens in inoculum consisted of *Methanosaeta* (25.07%), *Methanofastidiosum* (22.00%), *Methanoplasma* (18.07%), *Methanobacterium* (14.31%), and *RumEn_M2* (13.70%). In the FW-SDFW, FW-SH140, and FW-SH180 samples, *Methanoplasma* was the most dominant methanogen with slightly varying relative abundances from 47.57% to 68.64%, followed by *RumEn_M2* (12.56–30.86%) and *Methanobacterium* (3.92–17.18%). However, the most dominant methanogen in the FW-Water was *Methanobacterium* (45.13%). Therefore, the addition of SDFW, SH140, and SH180 changed the dominant methanogens.

Methanoplasma and *RumEn_M2* are common hydrogenotrophic methanogens [55]. *Methanoplasma* can promote acidification and methanation, especially in anaerobic digestion systems with a high organic loading rate [56]. The abundance of *Methanoplasma* and *RumEn_M2* explained the abundant CH_4 collection (higher than 290 mL per g COD) in FW-SDFW, FW-SH140, and FW-SH180. *Methanobacterium* is a hydrogenotrophic methanogen that produces CH_4 from H_2 and CO_2. During the acidogenesis stage, the *Methanobacterium* proportion was 3.92% in FW-SDFW, although it increased to 9.67% and 17.18% in FW-SH140 and FW-SH180, respectively. The same trend was observed in the methanogenesis stage. Interestingly, no CH_4 was produced in the FW-Water samples, although *Methanobacterium* was the most dominant methanogen. This result may be attributable to the acidic environment in the FW-Water samples. The pH of the FW-Water samples was approximately 5.21, at which very few microorganisms except *Methanobacterium* can survive [57].

Notably, *Methanosarcina* was undetectable in the inoculum, FW-Water, or FW-SDFW, but was observed in FW-SH140 and FW-SH180. The relative abundances of *Methanosarcina* in FW-SH140

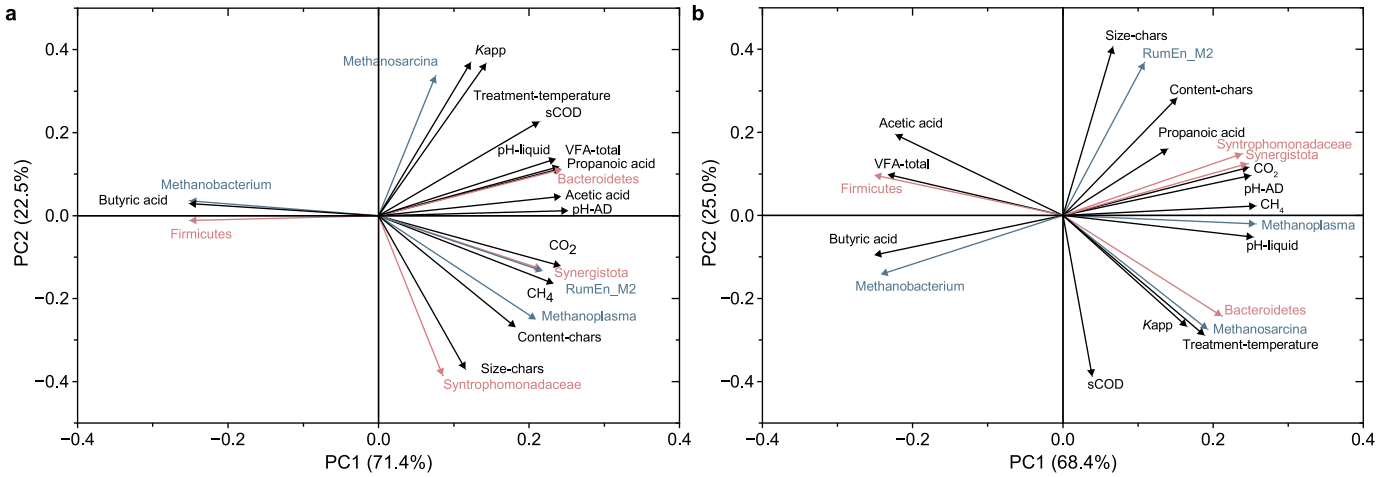

Fig. 7. Principal component analysis (PCA) between parameters of the added liquid and the performance of anaerobic co-digestion at acidogenesis (**a**) and methanogenesis (**b**) stages.

and FW-180 in the acidogenesis stage were 0.07% and 0.09%, which increased to 5.13% and 4.93% in the methanogenesis stage, respectively. *Methanosarcina* is a mixotrophic methanogen that can produce CH_4 through acetoclastic methanogenesis and syntrophic acetate oxidation coupled with the hydrogenotrophic methanogenesis pathway [58]. *Methanosarcina* can accept electrons directly from conductive materials and reduce propionate directly to CH_4 [58,59]. Moreover, *Methanosarcina* can promote propionic acid degradation and exhibits a syntrophic relationship with many syntrophic bacteria, such as *Sytrophomonas* of the Syntrophomonadaceae family, which can help promote CH_4 production [1,60]. In this study, the relative abundances of Syntrophomonadaceae in FW-SH140 and FW-SH180 in the acidogenesis stage were only 0.09% and 0.12%, which increased to 7.14% and 5.44% in the methanogenesis stage, respectively (Fig. S5), consistent with the trend of *Methanosarcina*. The enrichment of Syntrophomonadaceae and *Methanosarcina* in the methanogenesis stage may promote the conversion of propionic acid to CH_4. The microbial community analysis indicated that the self-generated hydrochars in the HTT liquid could increase the abundance of *Methanosarcina,* and their syntrophic bacteria. The abundance increases of Synergistota, Syntrophomonadaceae, and *Methanosarcina* was probably caused by the increase of the electron transferring rate between the two microbial communities after the addition of HTT liquid. It should be noted that no direct evidence was provided in this study to demonstrate the increase in microbial electron transferring activity, which should be further explored in future studies.

3.4. Possible promoting mechanism based on PCA analysis

The possible interrelation was investigated via PCA between parameters of the added liquid (deionized water, SDFW, SH140, and SH180) and the performance of anaerobic co-digestion at the acidogenesis and methanogenesis stages (Fig. 7). The first principal axis (PC1) was associated with the pH of the anaerobic co-digestion system or the variables that can influence the pH of anaerobic co-digestion, such as VFAs and the pH of added liquid. The second principal axis (PC2) was associated with the electron transferring performance, including k_{app}, *Methanosarcina*, and Syntrophomonadaceae. The two principal components can explain 93.9% and 93.4% of data variability values, illustrating the associations between these principal axes and the variables and experimental conditions.

As shown in Fig. 7a, the pH of the added liquid was highly correlated to the pH of the anaerobic digestion system, the VFAs production, and the abundance of Bacteroidetes during the acidogenesis stage. As described in Section 3.1.1, the pH of FW-Water sharply decreased to 5.21 during anaerobic digestion, but the pH of FW-SDFW, FW-SH140, and FW-SH180 was stable at approximately 7.2 with adding SDFW (pH = 7.76), SH140 (pH = 8.26) and SH180 (pH = 8.13). No inhibiting microbial activity in FW-SDFW, FW-SH140, and FW-SH180 was observed. These results indicated that the DFW and HTT liquid may act as a buffer to keep the anaerobic co-digestion system in a favorable pH range. Tian et al. [61] also observed a similar pH buffering effect of the HTT effluents from wheat straw on the anaerobic co-digestion with the waste-activated sludge. Moreover, the pH buffering effect possibly promoted the growth of Bacteroidetes and the generation of VFAs in the anaerobic co-digestion. The positive correlation between the pH of the anaerobic digestion system and cumulative CH_4 production for the methanogenesis stage (Fig. 7b) indicated the favorable pH range in FW-SDFW, FW-SH140, and FW-SH180 contributed to CH_4 conversion. In addition, a positive correlation was observed between the HTT temperature and the sCOD for the acidogenesis stage of anaerobic digestion (Fig. 7b). This may be due to the HTT process accelerating the decomposition of organic matter and improving their biodegradability [9]. It is also evidenced that less organic matter remained in the supernatant and solid residue after anaerobic co-digestion of FW-SH140 and FW-SH180 compared to that of FW-Water and FW-SDFW (Table 1).

During the methanogenesis stages of anaerobic co-digestion, the k_{app} has a positive correlation with the relative abundance of *Methanosarcina*, and slight positive correlations with Syntrophomonadaceae and Synergistota (Fig. 7b). The relative abundance of *Methanosarcina*, Syntrophomonadaceae, and Synergistota were increased with the addition of HTT liquid (Figs. 5 and 6), which is probably due to the increase of k_{app} caused by self-generated hydrochars. Usman et al. [21] and Shi et al. [22] have reported that hydrochars can improve electron transferring performance of anaerobic digestion system. For this study, the hydrochars with higher C content and abundant oxygen-containing functional groups were self-generated during HTT. These characteristics of the self-generated hydrochars can help them to donate and accept electrons, thereby facilitating direct interspecies electron transfer during anaerobic digestion [20,45,46].

As suggested above, there are two possible aspects for the HTT

liquid to promote methane production. One is the pH buffering effect of alkaline liquid, and the other is the promoting effect of self-generated hydrochars on direct interspecies electron transfer. The study is expected to provide novel insights regarding the mechanism of the anaerobic co-digestion of HTT liquid and food waste. However, a synergistic analysis of proteomics and metatranscriptomics in microbiology is necessary to clarify the underlying mechanism of HTT liquid in promoting CH_4 conversion from the metabolic and molecular levels.

4. Conclusions

Anaerobic co-digestion of the HTT liquid fraction and food waste is an efficient technique to valorize solid and liquid waste. In the anaerobic co-digestion system, CH_4 production yield and rate are enhanced. The HTT liquid generated at 180 °C can better promote CH_4 production than those generated at 140 °C. The maximum CH_4 production is 331.61 mL per g COD, and 79.4% of the organic matter is converted to CH_4. The anaerobic digestion conditions of pure food waste are volatile. Alkaline DFW liquid and it's HTT liquid can maintain the pH of the anaerobic co-digestion system at approximately 7, which is favorable for microbial growth. Furthermore, the organic matter in the digestate liquid is carbonized during HTT. The self-generated hydrochars, rich in carbon- and oxygen-containing functional groups, can accelerate the electron transferring rate, hence promoting the growth of syntrophic bacteria and methanogens.

CRediT authorship contribution statement

Mingshuai Shao: data analysis, original draft; **Chao Zhang:** data analysis, review, and editing; **Xue Wang:** Methodology and Investigation; **Ning Wang:** Methodology and Resources; **Qindong Chen:** Methodology and Investigation; **Guangyu Cui:** Methodology; **Qiyong Xu:** review and editing, Funding acquisition, project administration, and supervision.

Declaration of competing interest

The authors declare that they have no known competing financial interests or personal relationships that could have appeared to influence the work reported in this work.

Acknowledgments

This work was financially supported by the Shenzhen Fundamental Research Program (No. GXWD20201231165807007-20220724202837001).

Appendix A. Supplementary data

Supplementary data to this article can be found online at https://doi.org/10.1016/j.ese.2023.100239.

References

[1] Y. Li, Z. Chen, Y. Peng, W. Huang, J. Liu, V. Mironov, S. Zhang, Deeper insights into the effects of substrate to inoculum ratio selection on the relationship of kinetic parameters, microbial communities, and key metabolic pathways during the anaerobic digestion of food waste, Water Res. 217 (2022), 118440, https://doi.org/10.1016/j.watres.2022.118440.

[2] C.P.C. Bong, L.Y. Lim, C.T. Lee, J.J. Klemeš, C.S. Ho, W.S. Ho, The characterisation and treatment of food waste for improvement of biogas production during anaerobic digestion – a review, J. Clean. Prod. 172 (2018) 1545–1558, https://doi.org/10.1016/j.jclepro.2017.10.199.

[3] J. Lu, S. Xu, Post-treatment of food waste digestate towards land application: a review, J. Clean. Prod. 303 (2021), 127033, https://doi.org/10.1016/j.jclepro.2021.127033.

[4] N. Wang, D. Huang, M. Shao, R. Sun, Q. Xu, Use of activated carbon to reduce ammonia emissions and accelerate humification in composting digestate from food waste, Bioresour. Technol. 347 (2022), 126701, https://doi.org/10.1016/j.biortech.2022.126701.

[5] C. Jin, S. Sun, D. Yang, W. Sheng, Y. Ma, W. He, G. Li, Anaerobic digestion: an alternative resource treatment option for food waste in China, Sci. Total Environ. 779 (2021), 146397, https://doi.org/10.1016/j.scitotenv.2021.146397.

[6] M. Usman, H. Chen, K. Chen, S. Ren, J.H. Clark, J. Fan, G. Luo, S. Zhang, Characterization and utilization of aqueous products from hydrothermal conversion of biomass for bio-oil and hydro-char production: a review, Green Chem. 21 (7) (2019) 1553–1572, https://doi.org/10.1039/c8gc03957g.

[7] C. Li, J. Li, L. Pan, X. Zhu, S. Xie, G. Yu, Y. Wang, X. Pan, G. Zhu, I. Angelidaki, Treatment of digestate residues for energy recovery and biochar production: from lab to pilot-scale verification, J. Clean. Prod. 265 (2020), 121852, https://doi.org/10.1016/j.jclepro.2020.121852.

[8] R. Chen, X. Dai, B. Dong, Decrease the effective temperature of hydrothermal treatment for sewage sludge deep dewatering: mechanistic of tannic acid aided, Water Res. 217 (2022), 118450, https://doi.org/10.1016/j.watres.2022.118450.

[9] C. Zhang, M. Shao, H. Wu, N. Wang, Q. Chen, Q. Xu, Management and valorization of digestate from food waste via hydrothermal, Resour. Conserv. Recycl. 171 (2021), 105639, https://doi.org/10.1016/j.resconrec.2021.105639.

[10] L. Wang, A. Li, Y. Chang, Relationship between enhanced dewaterability and structural properties of hydrothermal sludge after hydrothermal treatment of excess sludge, Water Res. 112 (2017) 72–82, https://doi.org/10.1016/j.watres.2017.01.034.

[11] F. Lü, Q. Zhou, D. Wu, T. Wang, L. Shao, P. He, Dewaterability of anaerobic digestate from food waste: relationship with extracellular polymeric substances, Chem. Eng. J. 262 (2015) 932–938, https://doi.org/10.1016/j.cej.2014.10.051.

[12] A. Lee, D. Lewis, T. Kalaitzidis, P. Ashman, Technical issues in the large-scale hydrothermal liquefaction of microalgal biomass to biocrude, Curr. Opin. Biotechnol. 38 (2016) 85–89, https://doi.org/10.1016/j.copbio.2016.01.004.

[13] C. Aragon-Briceño, A. Pożarlik, E. Bramer, G. Brem, S. Wang, Y. Wen, W. Yang, H. Pawlak-Kruczek, Ł. Niedźwiecki, A. Urbanowska, K. Mościcki, M. Płoszczyca, Integration of hydrothermal carbonization treatment for water and energy recovery from organic fraction of municipal solid waste digestate, Renew. Energy 184 (2022) 577–591, https://doi.org/10.1016/j.renene.2021.11.106.

[14] E. Monfet, G. Aubry, A.A. Ramirez, Nutrient removal and recovery from digestate: a review of the technology, Biofuels 9 (2) (2017) 247–262, https://doi.org/10.1080/17597269.2017.1336348.

[15] C. Zhang, M. Shao, H. Wu, N. Wang, X. Wang, Q. Wang, Q. Xu, Mechanism insights into hydrothermal dewatering of food waste digestate for products valorization, Sci. Total Environ. 804 (2022), 150145, https://doi.org/10.1016/j.scitotenv.2021.150145.

[16] M. Lucian, M. Volpe, F. Merzari, D. Wust, A. Kruse, G. Andreottola, L. Fiori, Hydrothermal carbonization coupled with anaerobic digestion for the valorization of the organic fraction of municipal solid waste, Bioresour. Technol. 314 (2020), 123734, https://doi.org/10.1016/j.biortech.2020.123734.

[17] T. Yuan, Y. Cheng, Z. Zhang, Z. Lei, K. Shimizu, Comparative study on hydrothermal treatment as pre- and post-treatment of anaerobic digestion of primary sludge: focus on energy balance, resources transformation and sludge dewaterability, Appl. Energy 239 (1) (2019) 171–180, https://doi.org/10.1016/j.apenergy.2019.01.206.

[18] M.A. De la Rubia, J.A. Villamil, J.J. Rodriguez, R. Borja, A.F. Mohedano, Mesophilic anaerobic co-digestion of the organic fraction of municipal solid waste with the liquid fraction from hydrothermal carbonization of sewage sludge, Waste Manag. 76 (2018) 315–322, https://doi.org/10.1016/j.wasman.2018.02.046.

[19] E. Suarez, M. Tobajas, A.F. Mohedano, M.A. de la Rubia, Energy recovery from food waste and garden and park waste: anaerobic co-digestion versus hydrothermal treatment and anaerobic co-digestion, Chemosphere 297 (2022), 134223, https://doi.org/10.1016/j.chemosphere.2022.134223.

[20] S. Ren, M. Usman, D.C.W. Tsang, S. O-Thong, I. Angelidaki, X. Zhu, S. Zhang, G. Luo, Hydrochar-facilitated anaerobic digestion: evidence for direct interspecies electron transfer mediated through surface oxygen-containing functional groups, Environ. Sci. Technol. 54 (9) (2020) 5755–5766, https://doi.org/10.1021/acs.est.0c00112.

[21] M. Usman, Z. Shi, S. Ren, H.H. Ngo, G. Luo, S. Zhang, Hydrochar promoted anaerobic digestion of hydrothermal liquefaction wastewater: focusing on the organic degradation and microbial community, Chem. Eng. J. 399 (2020), 125766, https://doi.org/10.1016/j.cej.2020.125766.

[22] Z. Shi, M. Usman, J. He, H. Chen, S. Zhang, G. Luo, Combined microbial transcript and metabolic analysis reveals the different roles of hydrochar and biochar in promoting anaerobic digestion of waste activated sludge, Water Res. 205 (2021), 117679, https://doi.org/10.1016/j.watres.2021.117679.

[23] T. Yuan, S. Bian, J.H. Ko, J. Liu, X. Shi, Q. Xu, Exploring the roles of zero-valent iron in two-stage food waste anaerobic digestion, Waste Manag. 107 (2020) 91–100, https://doi.org/10.1016/j.wasman.2020.04.004.

[24] R.J. Wakeman, Separation technologies for sludge dewatering, J. Hazard Mater. 144 (2007) 614–619, https://doi.org/10.1016/j.jhazmat.2007.01.084.

[25] F. Raposo, M.A. De la Rubia, V. Fernández-Cegrí, R. Borja, Anaerobic digestion of solid organic substrates in batch mode: an overview relating to methane

yields and experimental procedures, Renew. Sustain. Energy Rev. 16 (1) (2012) 861–877, https://doi.org/10.1016/j.rser.2011.09.008.
[26] A. Rozzi, E. Remigi, Methods of assessing microbial activity and inhibition under anaerobic conditions: a literature review, Rev. Environ. Sci. Biotechnol. 3 (2) (2004) 93–115, https://doi.org/10.1007/s11157-004-5762-z.
[27] L. Yue, J. Cheng, H. Zhang, L. Yuan, J. Hua, H. Dong, Y. Li, J. Zhou, Inhibition of N-Vanillylnonanamide in anaerobic digestion of lipids in food waste: microorganisms damage and blocked electron transfer, J. Hazard Mater. 399 (2020), 123098, https://doi.org/10.1016/j.jhazmat.2020.123098.
[28] C.M. Braguglia, A. Gallipoli, A. Gianico, P. Pagliaccia, Anaerobic bioconversion of food waste into energy: a critical review, Bioresour. Technol. 248 (2018) 37–56, https://doi.org/10.1016/j.biortech.2017.06.145.
[29] APHA, Standard Methods for the Examination of Water and Wastewater, twenty-first ed., American Public Health Association, Washington, D.C, 2005. https://ajph.aphapublications.org.
[30] E.Y. Lim, H. Tian, Y. Chen, K. Ni, J. Zhang, Y. Tong, Methanogenic pathway and microbial succession during start-up and stabilization of thermophilic food waste anaerobic digestion with biochar, Bioresour. Technol. 314 (2020), 123751, https://doi.org/10.1016/j.biortech.2020.123751.
[31] Q. Yin, S. Yang, Z. Wang, L. Xing, G. Wu, Clarifying electron transfer and metagenomic analysis of microbial community in the methane production process with the addition of ferroferric oxide, Chem. Eng. J. 333 (2018) 216–225, https://doi.org/10.1016/j.cej.2017.09.160.
[32] J. Li, L. Xiao, S. Zheng, Y. Zhang, M. Luo, C. Tong, H. Xu, Y. Tan, J. Liu, O. Wang, F. Liu, A new insight into the strategy for methane production affected by conductive carbon cloth in wetland soil: beneficial to acetoclastic methanogenesis instead of CO2 reduction, Sci. Total Environ. 643 (2018) 1024–1030, https://doi.org/10.1016/j.scitotenv.2018.06.271.
[33] Y. Yuan, S. Zhou, N. Xu, L. Zhuang, Electrochemical characterization of anodic biofilms enriched with glucose and acetate in single-chamber microbial fuel cells, Colloids Surf., B 82 (2) (2011) 641–646, https://doi.org/10.1016/j.colsurfb.2010.10.015.
[34] K.G. Latham, I. Kozyatnyk, J. Figueira, M. Carlborg, E. Rosenbaum, S. Jansson, Self-generation of low ash carbon microspheres from the hydrothermal supernatant of anaerobic digestate: formation insights and supercapacitor performance, Adv. Chem. Eng. 6 (2021), 100097, https://doi.org/10.1016/j.ceja.2021.100097.
[35] K.L. Sainani, Introduction to principal components analysis, Phys. Med. Rehabil. 6 (3) (2014) 275–278, https://doi.org/10.1016/j.pmrj.2014.02.001.
[36] S. Mehariya, A.K. Patel, P.K. Obulisamy, E. Punniyakotti, J.W.C. Wong, Co-digestion of food waste and sewage sludge for methane production: current status and perspective, Bioresour. Technol. 265 (2018) 519–531, https://doi.org/10.1016/j.biortech.2018.04.030.
[37] H. Fisgativa, A. Tremier, P. Dabert, Characterizing the variability of food waste quality: a need for efficient valorisation through anaerobic digestion, Waste Manag. 50 (2016) 264–274, https://doi.org/10.1016/j.wasman.2016.01.041.
[38] Y. Qin, L. Li, J. Wu, B. Xiao, T. Hojo, K. Kubota, J. Cheng, Y. Li, Co-production of biohydrogen and biomethane from food waste and paper waste via recirculated two-phase anaerobic digestion process: bioenergy yields and metabolic distribution, Bioresour. Technol. 276 (2019) 325–334, https://doi.org/10.1016/j.biortech.2019.01.004.
[39] S. Dutta, M. He, X. Xiong, D.C.W. Tsang, Sustainable management and recycling of food waste anaerobic digestate: a review, Bioresour. Technol. 341 (2021), 125915, https://doi.org/10.1016/j.biortech.2021.125915.
[40] K.R. Parmar, A.B. Ross, Integration of hydrothermal carbonisation with anaerobic digestion; opportunities for valorisation of digestate, Energies 12 (9) (2019), https://doi.org/10.3390/en12091586.
[41] Z. Cao, D. Jung, M.P. Olszewski, P.J. Arauzo, A. Kruse, Hydrothermal carbonization of biogas digestate: effect of digestate origin and process conditions, Waste Manag. 100 (2019) 138–150, https://doi.org/10.1016/j.wasman.2019.09.009.
[42] A. Kruse, T. Zevaco, Properties of hydrochar as fnction of feedstock, reaction conditions and post-treatment, Energies 11 (3) (2018) 674–686, https://doi.org/10.3390/en11030674.
[43] S.A. Opatokun, T. Kan, A. Al Shoaibi, C. Srinivasakannan, V. Strezov, Characterization of food waste and its digestate as feedstock for thermochemical processing, Energ, Fuel 30 (3) (2015) 1589–1597, https://doi.org/10.1021/acs.energyfuels.5b02183.
[44] A. Funke, F. Ziegler, Hydrothermal carbonization of biomass: a summary and discussion of chemical mechanisms for process engineering, Biofuel. Bioprod. Bior. 4 (2) (2010) 160–177, https://doi.org/10.1002/bbb.198.
[45] S. Wu, G. Fang, Y. Wang, Y. Zheng, C. Wang, F. Zhao, D.P. Jaisi, D. Zhou, Redox-active oxygen-containing functional groups in activated carbon facilitate microbial reduction of ferrihydrite, Environ. Sci. Technol. 51 (17) (2017) 9709–9717, https://doi.org/10.1021/acs.est.7b01854.
[46] A. Kappler, M.L. Wuestner, A. Ruecker, J. Harter, M. Halama, S. Behrens, Biochar as an electron shuttle between bacteria and Fe(III) minerals, Environ. Sci. Technol. Lett. 1 (8) (2014) 339–344, https://doi.org/10.1021/ez5002209.
[47] Q. An, D. Chen, H. Chen, X. Yue, L. Wang, Modification of hydro-chars by non-thermal plasma to enhance co-anaerobic digestion and degradation of sewage sludge pyrolysis oil, J. Environ. Manag. 307 (2022), 114531, https://doi.org/10.1016/j.jenvman.2022.114531.
[48] R. Lin, J. Cheng, L. Ding, J.D. Murphy, Improved efficiency of anaerobic digestion through direct interspecies electron transfer at mesophilic and thermophilic temperature ranges, Chem. Eng. J. 350 (2018) 681–691, https://doi.org/10.1016/j.cej.2018.05.173.
[49] L. Wu, Y. Yang, S. Chen, M. Zhao, Z. Zhu, S. Yang, Y. Qu, Q. Ma, Z. He, J. Zhou, Q. He, Long-term successional dynamics of microbial association networks in anaerobic digestion processes, Water Res. 104 (2016) 1–10, https://doi.org/10.1016/j.watres.2016.07.072.
[50] J.W. Lim, J.A. Chiam, J. Wang, Microbial community structure reveals how microaeration improves fermentation during anaerobic co-digestion of brown water and food waste, Bioresour. Technol. 171 (2014) 132–138, https://doi.org/10.1016/j.biortech.2014.08.050.
[51] Y. Zhong, J. He, P. Zhang, X. Zou, X. Pan, J. Zhang, Effects of different particle size of zero-valent iron (ZVI) during anaerobic digestion: performance and mechanism from genetic level, Chem. Eng. J. 435 (2022), 134977, https://doi.org/10.1016/j.cej.2022.134977.
[52] D. Rivie`re, V. Desvignes, E. Pelletier, S. Chaussonnerie, S. Guermazi, J. Weissenbach, T. Li, P. Camacho, A. Sghir, Towards the definition of a core of microorganisms involved in anaerobic digestion of sludge, ISME J. 3 (6) (2009) 700–714, https://doi.org/10.1038/ismej.2009.2.
[53] S. Yang, Z. Chen, Q. Wen, Impacts of biochar on anaerobic digestion of swine manure: methanogenesis and antibiotic resistance genes dissemination, Bioresour. Technol. 324 (2021), 124679, https://doi.org/10.1016/j.biortech.2021.124679.
[54] K.M. Ritalahti, S.D. Justicia-Leon, K.D. Cusick, N. Ramos-Hernandez, M. Rubin, J. Dornbush, F.E. Loffler, Sphaerochaeta globosa gen. nov., sp. nov. and Sphaerochaeta pleomorpha sp. nov., free-living, spherical spirochaetes, Int. J. Syst. Evol. Microbiol. 62 (Pt 1) (2012) 210–216, https://doi.org/10.1099/ijs.0.023986-0.
[55] Z. Xie, Q. Cao, Y. Chen, Y. Luo, X. Liu, D. Li, The biological and abiotic effects of powdered activated carbon on the anaerobic digestion performance of cornstalk, Bioresour. Technol. 343 (2022), 126072, https://doi.org/10.1016/j.biortech.2021.126072.
[56] K. Lang, J. Schuldes, A. Klingl, A. Poehlein, R. Daniel, A. Brune, New mode of energy metabolism in the seventh order of methanogens as revealed by comparative genome analysis of "candidatus Methanoplasma termitum, Appl. Environ. Microbiol. 81 (4) (2015) 1338–1352, https://doi.org/10.1128/aem.03389-14.
[57] G.T. Tejerizo, Y.S. Kim, I. Maus, D. Wibberg, A. Winkler, S. Off, A. Puhler, P. Scherer, A. Schluter, Genome sequence of Methanobacterium congolense strain Buetzberg, a hydrogenotrophic, methanogenic archaeon, isolated from a mesophilic industrial-scale biogas plant utilizing bio-waste, J. Biotechnol. 247 (2017) 1–5, https://doi.org/10.1016/j.jbiotec.2017.02.015.
[58] J. De Vrieze, T. Hennebel, N. Boon, W. Verstraete, Methanosarcina: the rediscovered methanogen for heavy duty biomethanation, Bioresour. Technol. 112 (2012) 1–9, https://doi.org/10.1016/j.biortech.2012.02.079.
[59] Y. Lei, L. Wei, T. Liu, Y. Xiao, Y. Dang, D. Sun, D.E. Holmes, Magnetite enhances anaerobic digestion and methanogenesis of fresh leachate from a municipal solid waste incineration plant, Chem. Eng. J. 348 (2018) 992–999, https://doi.org/10.1016/j.cej.2018.05.060.
[60] J. Ma, J. Pan, L. Qiu, Q. Wang, Z. Zhang, Biochar triggering multipath methanogenesis and subdued propionic acid accumulation during semi-continuous anaerobic digestion, Bioresour. Technol. 293 (2019), 122026, https://doi.org/10.1016/j.biortech.2019.122026.
[61] W. Tian, Y. Chen, Y. Shen, C. Zhong, M. Gao, D. Shi, Q. He, L. Gu, Effects of hydrothermal pretreatment on the mono- and co-digestion of waste activated sludge and wheat straw, Sci. Total Environ. 732 (2020), 139312, https://doi.org/10.1016/j.scitotenv.2020.139312.